



Article

Analysis of the Long-Term Characteristics of BDS On-Orbit Satellite Atomic Clock: Since BDS-3 Was Officially Commissioned

Yifeng Liang, Jiangning Xu, Miao Wu and Fangneng Li *

School of Electrical Engineering, Naval University of Engineering, Wuhan 430033, China

* Correspondence: fangneng_li@126.com; Tel.: +86-159-7298-2496

Abstract: Satellite atomic clocks are the key elements for position, navigation, and timing services of the Global navigation satellite system (GNSS); it is necessary to research the characteristics of BDS-3 on-orbit satellite atomic clocks for their further optimization. In this study, clock offset data with a duration of 620 days since BDS-3 was officially commissioned were applied to long-term characteristic analysis. To begin with, the precision clock offset data of Deutsches geoforschungs zentrum (GFZ) processed by a MAD-based method were used as reliable test data. Herein, the working principle and main characteristics of satellite atomic clocks are analyzed and discussed, and thus, a comprehensive long-term characteristic analysis scheme is designed. On this basis, the performance indicators—mainly including physical parameters, periodic characteristics, frequency drift rate, frequency accuracy, frequency stability—were calculated and analyzed respectively, revealing the long-term characteristics of the BDS in orbit satellite atomic clocks during the test period. The results of experimental data testify that the performance of BDS-3 satellite atomic clocks is significantly superior to that of BDS-2, especially in terms of drift rate and frequency stability, and the performance of passive hydrogen maser (PHM) is generally superior to that of rubidium atomic frequency standards (RAFS). Within about half a year since BDS-3 was officially commissioned, the frequency stability of BDS-3 satellite atomic clock gradually improved and then reached the order of 10^{-15} , reflecting the effectiveness of system maintenance and inter-satellite link. Furthermore, some novel conclusions are drawn, such as the long-term period term of the fitting residual and drift rate, which may be caused by the earth's revolution.

Keywords: GNSS; BDS-3; satellite atomic clock; frequency stability; frequency drift rate



Citation: Liang, Y.; Xu, J.; Wu, M.; Li, F. Analysis of the Long-Term Characteristics of BDS On-Orbit Satellite Atomic Clock: Since BDS-3 Was Officially Commissioned. *Remote Sens.* **2022**, *14*, 4535. <https://doi.org/10.3390/rs14184535>

Academic Editors: Baocheng Zhang and Teng Liu

Received: 15 August 2022

Accepted: 1 September 2022

Published: 11 September 2022

Publisher's Note: MDPI stays neutral with regard to jurisdictional claims in published maps and institutional affiliations.



Copyright: © 2022 by the authors. Licensee MDPI, Basel, Switzerland. This article is an open access article distributed under the terms and conditions of the Creative Commons Attribution (CC BY) license (<https://creativecommons.org/licenses/by/4.0/>).

1. Introduction

The Beidou satellite navigation system has gone through the development stages of the experimental system (BDS-1), the regional system (BDS-2), and the global system (BDS-3) [1]. The service area of Beidou-1 was China, and Beidou-2 provided positioning, navigation, and timing (PNT) services for the Asia–Pacific region; there are still more than 10 Beidou-2 satellites in operation. From 2017 to 2020, the number of Beidou satellites increased rapidly, and finally, the main system of Beidou third-generation network (BDS-3) was officially commissioned in July 2020 and began to provide global services, marking the expansion of the scope of BDS services from the region to the world [2–4].

In terms of the working principle, BDS is a high-precision time synchronization system which requires stable frequency standards and a high-precision time scale to realize positioning and time service [5,6]. The satellite atomic clock, which could provide a stable on-satellite time, is an important payload for BDS satellites. The performance and working condition of satellite atomic clocks are directly related to the research on precision clock offset estimation and prediction technology, precision single-point positioning services, and so on. Therefore, it is of great significance to comprehensively evaluate the performance of BDS satellite atomic clocks and analyze their long-term on-orbit characteristics. In addition,

high-precision satellite atomic clocks are also key to precise point positioning (PPP) and are important in applications such as PPP-RTK [7–9].

With the development of GNSS, some analysis and discussion on the satellite atomic clocks of GPS, GLONASS, and Galileo systems have been carried out [10,11]. The on-orbit working characteristics of satellite atomic clocks has been obtained, including frequency stability level, periodic characteristics, and so on, which provide important reference for the operation of GNSS [12,13]. Overall, the frequency accuracy of GPS and Galileo satellite atomic clocks is in the range of 10^{-11} , the daily frequency drift rate is in the range of 10^{-14} , and the daily frequency stability is about $2\sim 5 \times 10^{-15}$ [14]. In terms of BDS, the existing research generally focuses on BDS-2 or some kinds of BDS-3 satellites. Hauschild et al. [15] and Wang et al. [16] studied the on-orbit performance characterization of BDS-2 and made a detailed analysis of the early BDS satellite atomic clock. Xie et al. [17–19] analyzed some parts of BDS-3 satellite atomic clocks from different angles, including precise orbit and clock determination for BDS-3 experimental satellites and performance of the BDS-3 experimental satellite PHM, mostly based on data over several months. However, a complete overview of the long-term and dynamic characteristics for the satellite atomic clock is lacking after the official commissioning of BDS-3 [2,20]. Since all on-orbit satellites provide PNT services for users, their atomic clocks should be studied and analyzed in detail, so as to analyze the overall working status of the system.

In order to accurately reflect the long-term operation characteristics of a BDS on-orbit satellite atomic clock and comprehensively evaluate its performance, this study was carried out on the basis of the precise clock offset data after the official commissioning of BDS-3. Firstly, in this paper, the characteristics of the original phase and average frequency are analyzed, and the MAD-based outlier detection method is used to provide clean experimental data for subsequent analysis. On this basis, the parameters and fitting residuals, long-term frequency drift rate, frequency accuracy, and frequency stability of the satellite atomic clocks are calculated; further to this, these indicators are discussed according to the system and atomic clock type. The fitting residual is processed by fast Fourier transform (FFT); the main periodic terms due to orbital operation are thus obtained. The approximately half-yearly periodic terms in the frequency drift rate are discussed, and some possible reasons are given. The performance of BDS-3 satellite atomic clocks with gradual improvement of frequency stability during the test period was analyzed; the results show that the daily frequency stability of BDS-3 satellite atomic clocks has reached a level superior to 8×10^{-15} after 2021.

The rest of this study is arranged as follows. Section 2 introduces the basic information of the BDS satellite and the clock offset data used in this study; the effectiveness of the data preprocessing method is shown. Section 3 introduces the working principle and model of the satellite atomic clock, and then the calculation method of the main indicators is described; thus, the long-term characteristic analysis process of the satellite atomic clock is given. In Section 4, the performance indicators of the BDS on-orbit satellite atomic clock are calculated, and the long-term variation characteristics from July 2020 are analyzed. Thereafter, in Section 5, the necessary overall analysis is given and some long-term characterization features are revealed, including the slowly changing periodic term of the fitting residual and frequency drift rate, the changing trend of the frequency stability, and so on. Eventually, Section 6 gives the conclusion of this study.

2. Experimental Data

2.1. Satellite Atomic Clock and Orbit Information of BDS

The BDS adopts a hybrid orbit, whose space segment is composed of several Geostationary Orbit (GEO), Inclined GeoSynchronous Orbit (IGSO), and Medium Earth Orbit (MEO) satellites. The main working clock of each satellite is RAFS or PHM; the details are shown in Table 1 (as of 12 March 2022).

Table 1. The information of BDS on-orbit satellites.

System	Orbit	PRN	Clock Types	Launch Date	Time (Day)		
BDS-2	GEO	C01	RAFS	17 May 2019	1030		
		C02	RAFS	25 October 2012	3425		
		C03	RAFS	12 June 2016	2099		
		C04	RAFS	31 October 2010	4150		
		C05	RAFS	24 February 2012	3669		
		C06	RAFS	31 July 2010	4242		
	IGSO	C07	RAFS	17 December 2010	4103		
		C08	RAFS	9 April 2011	3990		
		C09	RAFS	26 July 2011	3882		
		C10	RAFS	1 December 2011	3754		
		C13	RAFS	29 March 2016	2174		
		C16	RAFS	10 July 2018	1341		
		MEO	C11	RAFS	29 April 2012	3604	
			C12	RAFS	29 April 2012	3604	
BDS-3		C14	RAFS	18 September 2012	3462		
		C19	RAFS	5 November 2017	1588		
		C20	RAFS	5 November 2017	1588		
		C21	RAFS	12 February 2018	1489		
		C22	RAFS	12 February 2018	1489		
		C23	RAFS	29 July 2018	1322		
		C24	RAFS	29 July 2018	1322		
		MEO	C25	PHM	24 August 2018	1296	
			C26	PHM	24 August 2018	1296	
			C27	PHM	11 January 2018	1521	
			C28	PHM	11 January 2018	1521	
			C29	PHM	29 March 2018	1444	
			C30	PHM	29 March 2018	1444	
			C32	RAFS	19 September 2018	1270	
			C33	RAFS	19 September 2018	1270	
			IGSO	C34	PHM	15 October 2018	1244
				C35	PHM	15 October 2018	1244
		C36		RAFS	18 November 2018	1210	
		C37		RAFS	18 November 2018	1210	
		C41		PHM	16 December 2019	817	
		C42		PHM	16 December 2019	817	
		C43		PHM	23 November 2019	840	
		C44		PHM	23 November 2019	840	
		C45		RAFS	22 September 2019	902	
		C46		RAFS	22 September 2019	902	
		GEO	C38	PHM	20 April 2019	1057	
			C39	PHM	24 June 2019	992	
C40	PHM		4 November 2019	859			
C59	PHM		1 November 2018	1227			
C60	PHM		9 March 2020	733			
		C61	PHM	23 June 2020	627		

From Table 1, all of BDS-2 satellites were equipped with RAFS, most of which have been in operation for more than 2000 days and are gradually coming to the end of service. Correspondingly, most BDS-3 satellites containing new-type RAFS or PHM operate between 1000 and 2000 days, and are in stable operation. A few BDS-3 satellites have been launched within the last 1000 days and have not entered the stable operation stage. The composition of BDS satellite atomic clocks is so complex that various types need to be taken into account in the subsequent discussion [21].

2.2. Data Collection

Currently, the center for orbit determination in Europe (CODE), GFZ, GNSS research center of Wuhan University (WHU) (participating in the multi-GNSS experiment (MGEX)), and the International GNSS monitoring and assessment system (iGMAS) are the main research institutions of BDS precision clock offset, which obtain experimental data through Orbit Determination and Time Synchronization (ODTS) and publish it publicly [22]. Thus, GFZ precision clock offset data were selected mainly because of their high efficiency. As a result, BDS precision clock offset data of 620 days from 1 July 2020 to 12 March 2022 were collected; the data efficiency of every satellite clock is shown in Figure 1.

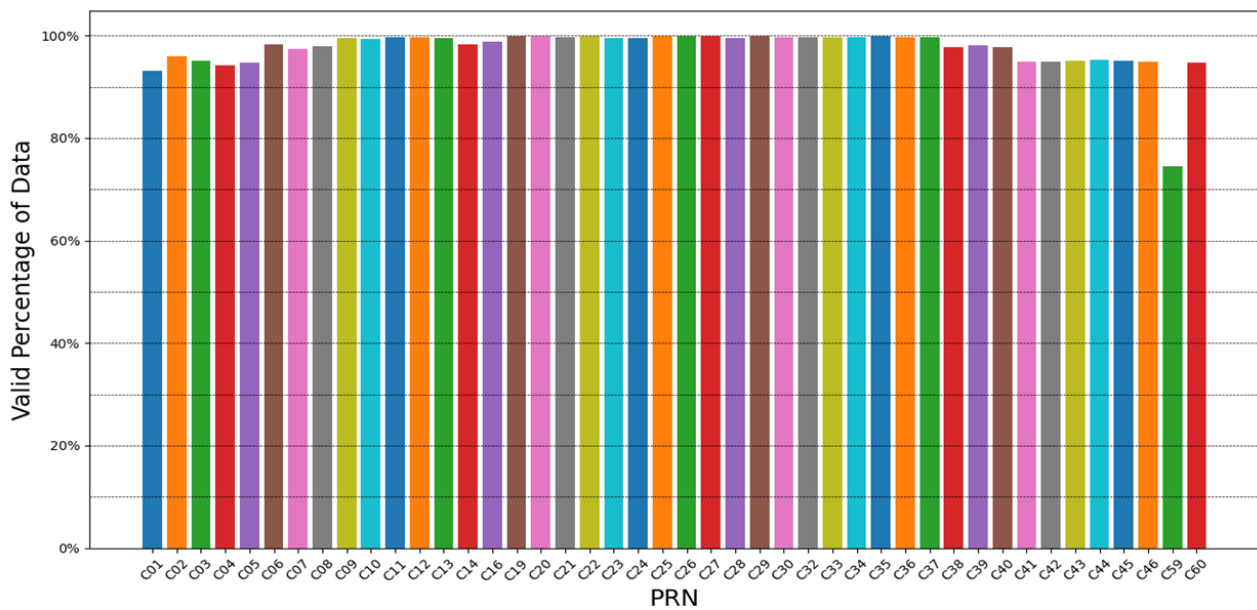


Figure 1. The Data Availability of BDS Satellites.

From Figure 1, the effective rate of BDS satellite atomic clock data released earlier and later is lower than the average value, which is caused by the fact that the operation is at the late or unstable stage. Specifically, the longest running retired satellite, C01, has a data efficiency of 93.09%; the four GEO clocks C02–C05 have a data efficiency of around 95%; and the MEO satellites C19–C37 of BDS-3 have a data efficiency of over 99.4%. The data efficiency of the C41–C60 satellites decreased because they have not been in operation long enough or are still in the on-orbit commissioning phase. Overall, the BDS-3 stable operation satellites (PRN C19–C40) have an average data efficiency of 99.45%, which is higher than the 97.43% of BDS-2 (PRN C01–C16).

2.3. Outlier Detection

As an experimental product, raw clock offset data usually contain outliers. The outlier detection method based on median absolute deviation (MAD) has robustness and adaptability, which is applicable to satellite atomic clock data with a large amount of data. The idea of outlier detection based on this method is to compare each frequency data with the median m of the frequency data sequence plus the sum of several times of MAD [14]; if the observed measurement is $|y_i| > (m + n \cdot \text{MAD})$, then it will be considered as outlier data, where $m = \text{Median}(y_i)$ and $\text{MAD} = \text{Median}(|y_i - m|/0.6745)$. In this study, initial phase data with relatively few effective positions were first converted to average frequency value, and then processed by MAD-based method; the outliers were set to null value, and finally, the clean frequency and phase data could be obtained [23].

Herein, C01 (BDS2-GEO), C27 (BDS3-MEO), and C37 (BDS3-IGSO) are used as examples to demonstrate the effectiveness of the above methods. The original phase data of the

three satellite atomic clocks are shown in Figure 2a, including rising and falling trends and multiple phase modulation operations. It is difficult to see the anomaly point from the phase data; thus, it is necessary to convert the phase data into frequency data, and then distinguish and eliminate the outliers. The corresponding frequency data are shown in Figure 2b, with multiple obvious outliers, as well as some gross errors that are difficult to observe. The frequency data processed by the MAD-based method is shown in Figure 2c, and the frequency trend of the three satellite atomic clocks is clearly visible. Therefore, the data processing approach taken is effective.

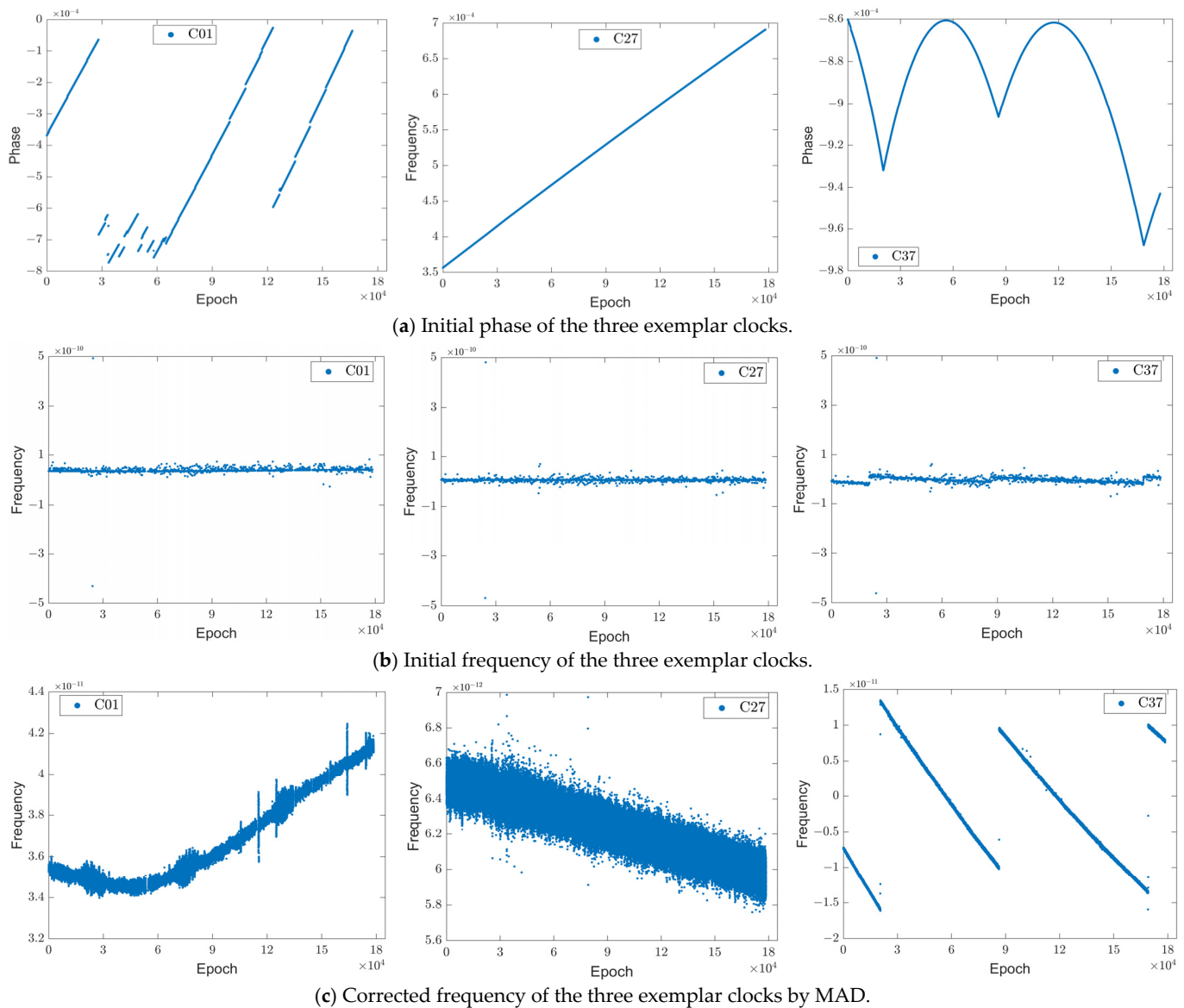


Figure 2. The effect of the outlier detection by MAD.

Figure 3 shows the comparison of the data efficiency of each satellite with the original data efficiency after using the MAD-based method to remove the outliers. MEO satellites of BDS-3 (C19–C37) have a raw data efficiency of no less than 99%, reflecting stable data quality. As a comparison, satellites that have been in service for only a short time (C41–C60) have a lower data efficiency, approximately equal to that of the early satellites of BDS-2. In detail, there were quite a lot data gaps in the early part of the statistical time interval, probably due to the fact that they are still in the commissioning phase, ultimately resulting in a high error rate of the data. For example, the error rate of C59 was 13.12%, which can seriously affect performance evaluation and analysis. The imperfection could be caused

by cycle slip, ionospheric bubbles, etc. The enumerated problems could be proved by dropouts in the C/N0 or by a similar characteristic. In order to ensure the preciseness of long-term characteristic analysis, the object of this study is specific to 35 satellite atomic clocks before PRN40.

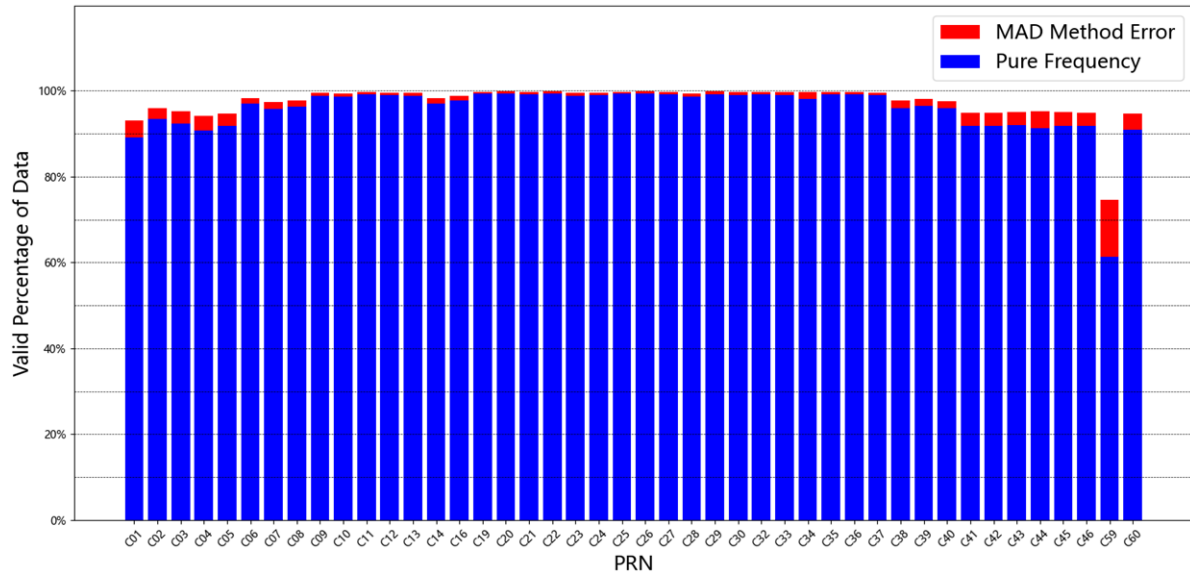


Figure 3. The Efficiency of the Clock Data after MAD Processing.

3. Analysis Methods

3.1. Satellite Atomic Clock Model and Noise Characteristic

The atomic clock model usually contains three parameters [24]:

- (1) Initial clock offset, a_0 , which represents the clock difference at time t_0 ;
- (2) Initial frequency offset, a_1 , which represents the relative frequency deviation at time t_0 ;
- (3) The frequency drift, a_2 , which represents the linear change of relative frequency deviation.

The atomic clock system can be considered as a numerical integrator that requires the three parameters mentioned above to form the oscillator, the schematic of which is shown in Figure 4. In terms of self-characterization and the influence of the working environment, the stochastic differential equation of a satellite atomic clock can be generally expressed as follows:

$$\Delta t(t) = a_0 + a_1 t + \frac{1}{2} a_2 t^2 + \frac{A}{2\pi f_0} \sin(2\pi f_0 + \varphi) \Big|_0^t + \sigma_1 W_1(t) + \sigma_2 \int_0^t W_2(s) ds + \sigma \varepsilon(t) \quad (1)$$

- $\frac{A}{2\pi f_0} \sin(2\pi f_0 + \varphi) \Big|_0^t$ expresses the periodic component in the phase, which was shown in the figure as environmental effects;
- $W_1(t)$, $W_2(t)$ are two independent Wiener processes as oscillator noise in the figure, representing the random component of the clock offset, respectively;
- $\sigma \varepsilon(t)$ is the observation noise.

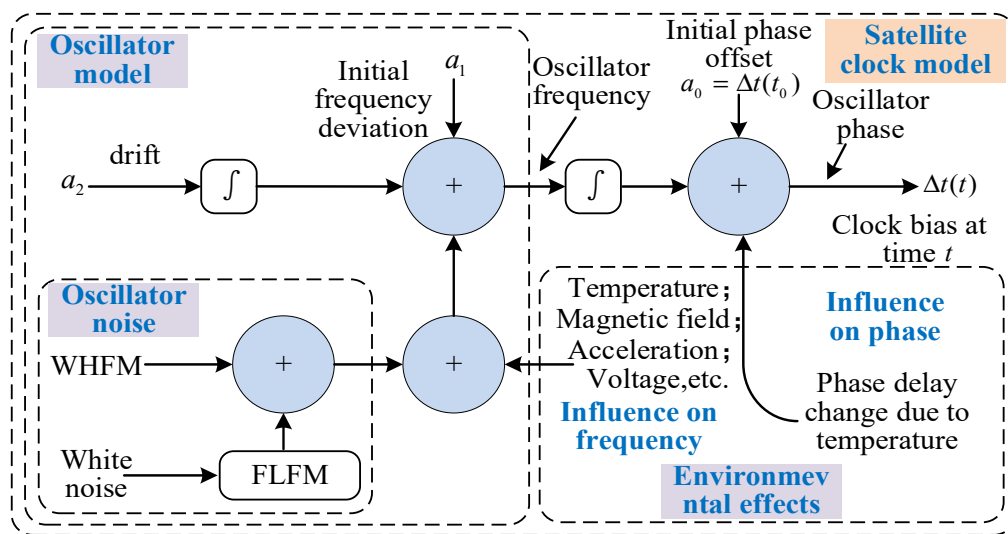


Figure 4. Satellite clock systematics model, including environmental and random effects.

In Equation (1), a_0, a_1, a_2 could be regarded as constant values in a short period of time; the periodic components produced by the orbital motion of the satellites usually have certain rules, especially for the main cycles. $W_1(t), W_2(t)$ usually represent white frequency modulation noise (WHFM) and flicker frequency modulation noise (FLFM), respectively. The stability equation of the clock offset, taking Allan variance as an example, can be expressed as follows:

$$\sigma_y^2(\tau) = 3\sigma^2/\tau^2 + \sigma_1^2/\tau + \frac{1}{3}\sigma_2^2\tau + \frac{1}{2}d^2\tau^2 + A^2\frac{\sin^4(\pi f_0\tau)}{(\pi f_0\tau)^2} \tag{2}$$

The main operational characteristics of a satellite atomic clock can be obtained from the above analysis, the phase output of which is determined by a combination of frequency, drift rate, periodic terms due to the environment, and noise. The relevant performance metrics include fitting residuals, frequency drift rate, and frequency accuracy. In addition, the noise characteristics are mainly determined by the frequency stability, and the periodic term can also cause an abnormal protrusion in frequency stability over a certain time period. The above analysis allows an intuitive understanding of the satellite atomic clock output pattern, enabling the design of a reasonable performance analysis scheme.

3.2. Main Performance Metrics of the Satellite Atomic Clock

(1) Fitting residual and periodic characteristic analysis

The frequency of BDS satellite clocks drift to some extent with frequency changes, especially for RAFS; therefore, their models are usually fitted by means of a quadratic polynomial model [25]:

$$L(t) = a_0 + \hat{a}_1t + \frac{1}{2}\hat{a}_2t^2 \tag{3}$$

where a_0 represents the initial clock offset, \hat{a}_1 is the estimated frequency offset, and \hat{a}_2 is the estimated frequency drift. Then, the fit residues can be obtained from Equations (1) and (3):

$$\Delta x(t) = x(t) - L(t) = (a_1 - \hat{a}_1)t + \frac{1}{2}(a_2 - \hat{a}_2)t^2 + \frac{A}{2\pi f_0} \sin(2\pi f_0 t + \varphi)|_0^t + \sigma_1 W_1(t) + \sigma_2 \int_0^t W_2(s)ds + \sigma \varepsilon(t) \tag{4}$$

It can be seen from Equation (4) that the fitted residual has the frequency and the clock drift component residual in the low-frequency part, the noise term in the high-frequency part, and the periodic term component in the middle part. Therefore, Fast

Fourier Transform (FFT) is used to identify and analyze satellite atomic clock period terms, with the following formula:

$$X(k) = \sum_{n=0}^{N-1} \Delta x(n) e^{-j \frac{2\pi}{N} kn} \quad (5)$$

where $X(k)$ is the spectral analysis sequence at epoch k , $\Delta x(n)$ is the clock data residuals fitted by quadratic polynomial, N is the number of residuals, j is an imaginary unit, and e is a mathematical constant.

(2) Frequency drift rate

Frequency drift rate is the ratio of the frequency offset before and after the operation of the satellite clock to the two-point sampling time interval, reflecting the frequency variation of the satellite clock within a certain period of time. The drift rate and daily drift rate are mainly used to measure the frequency drift of the atomic clock. The former is solved by short-term fitting of quadratic polynomial, and the latter is calculated by using longer-term data. For example, the frequency of one month is used for fitting, and the calculation formula is [26]:

$$D = \frac{\sum_{i=1}^N (y_i - \bar{y})(t_i - \bar{t})}{\sum_{i=1}^N (t_i - \bar{t})^2} \quad (6)$$

where y_i represents the frequency values at each moment, \bar{y} is the mean of the relative frequency value, t_i represents the moment of the measurement, and \bar{t} is equal to $\frac{1}{N} \sum_{i=1}^N t_i$.

(3) Frequency accuracy

Frequency accuracy is a measure of the deviation between the actual output frequency of a satellite clock and its reference frequency, showing the error of the satellite clock output frequency and the reference ground clock frequency. Usually, a frequency accuracy index can be obtained by fitting the phase data in a linear mode based on the least square principle [27]:

$$K_\tau = \frac{\sum_{i=1}^N (x_i - \bar{x})(t_i - \bar{t})}{\sum_{i=1}^N (t_i - \bar{t})^2} \quad (7)$$

where x_i represents the phase values at each moment, \bar{x} is the mean of the phase value, t_i represents the moment of the measurement, and \bar{t} is equal to $\frac{1}{N} \sum_{i=1}^N t_i$.

(4) Frequency stability

Frequency stability characterizes the ability of the same frequency source to stably produce a certain frequency over a certain period of time. The commonly used Allan variance belongs to the double-sampling treatment method and is greatly affected by the drift. To this end, the stability of BDS satellite atomic clocks was assessed by the triple-sampled Hadamard variance. To improve the utilization of the sampled data and the confidence of the calculation results, overlapping Hadamard variance is applied to calculate frequency stability, with the calculation equation of [28]:

$$H\sigma_y^2(\tau) = \frac{1}{6m^2(N-3m)} \sum_{i=1}^{N-3m} [x_{i+3m} - 3x_{i+2m} + 3x_{i+m} - x_i]^2 \quad (8)$$

where $\tau = m\tau_0$ is the smoothing time, x_i is the satellite clock offset data on the time series, N is the number of input clock offset data, and m is the smoothing factor.

3.3. Main Performance Metrics of the Satellite Atomic Clock

The exact procedures and steps of the evaluation process can be expressed as follows. BDS precise clock offset data are obtained by GFZ and converted into average frequency data; then, the outliers are removed by the MAD-based detection method. On this basis, the stability is obtained by overlapping Hadamard deviation, the frequency accuracy is solved by a linear model, the daily fitting residual and periodic term characteristics are obtained by a quadratic polynomial model, and the daily drift rate is solved by linear fitting of frequency data. Further to this, herein, the performance characterization is analyzed comprehensively. Finally, the necessary classification discussions are given according to clock, track, and system type. The evaluation process of main indicators is shown in Figure 5, and some technical details are described as follows:

- (1) During outlier detection, the daily frequency data are detected. The value of N is the empirical value, which is determined as 5 in this study. If the ratio of outliers in the day is lower than 20%, the processed data is used normally; otherwise, the data of the corresponding date will not be analyzed.
- (2) In terms of frequency drift rate, the drift rate and the daily drift rate are calculated to comprehensively reflect the short-term and long-term drift characteristics of the atomic clock.
- (3) The calculation of frequency stability requires large volumes of data to obtain high confidence levels. The frequency stability is calculated when the smoothing time is 10,200 s (smoothing factor of 34) and 86,400 s (smoothing factor of 288), representing the stability of 10,000 s and the daily stability, respectively. The stability index is given in different months to reflect its change trend.

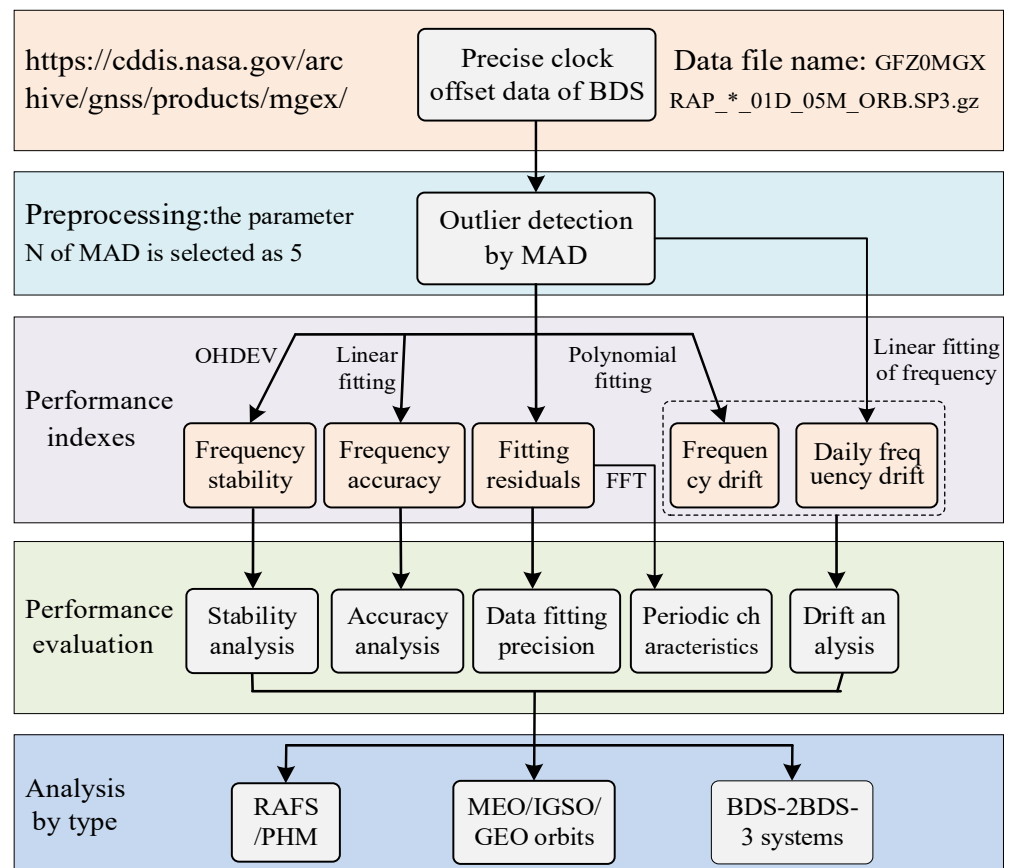


Figure 5. Evaluation process of main indicators.

4. Characteristics of the BDS Satellite Clock

4.1. Satellite Atomic Clock Model and Noise Characteristic

Herein, the approximate model and fitting residuals of a satellite atomic clock are first analyzed. The fitting results of the model are sampled here to obtain the daily fitting residual, and the spectrum of the residual sequence is analyzed for the periodic characteristics of the noise of the atomic clock. Figure 6 lists the fitting residual data of three atomic clocks from different orbits, with the PRN of C01 (GEO), C16 (IGSO), and C25 (MEO) satellites; the corresponding spectrums are also given.

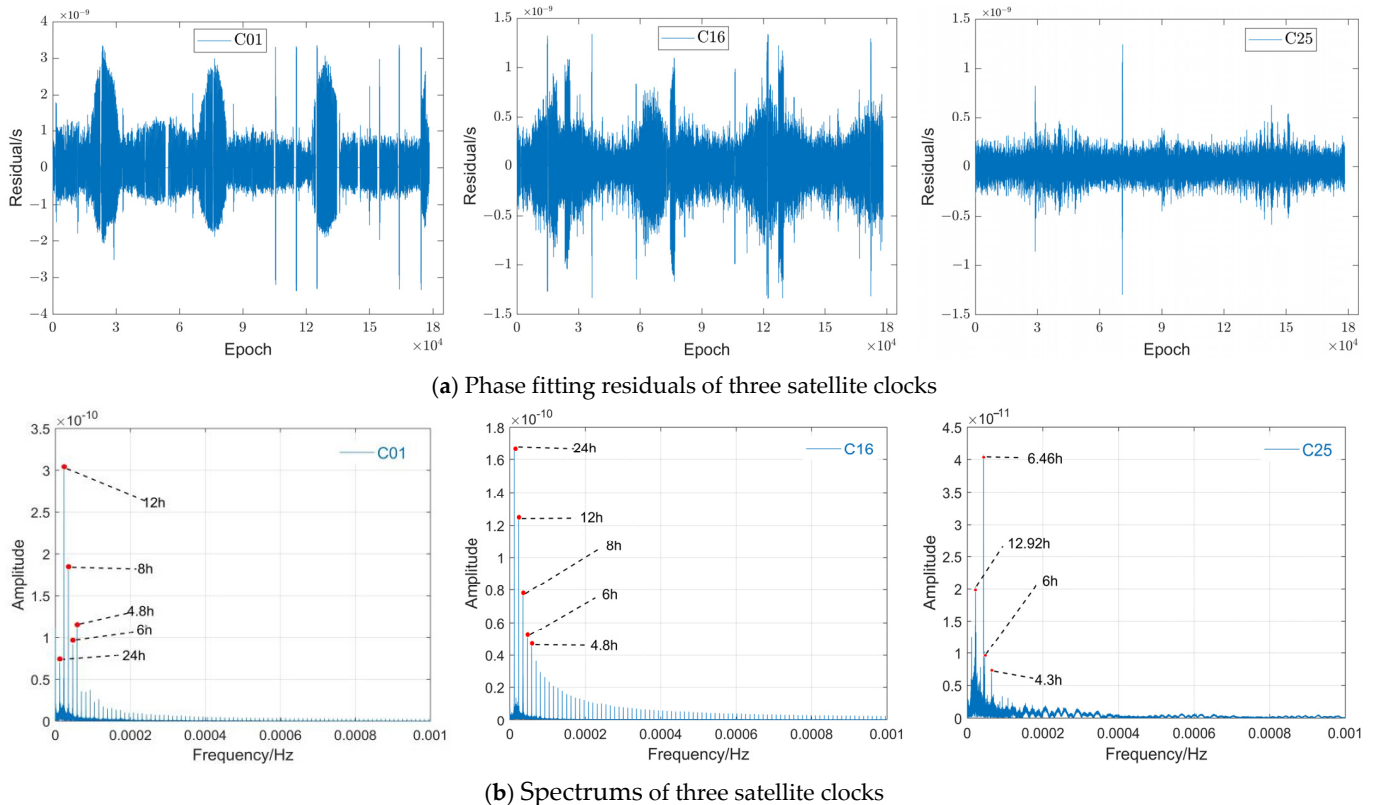


Figure 6. Residuals and spectrums of different satellite clocks.

In Figure 6, the RMS values of fitting residuals are 0.473 ns, 0.255 ns, and 0.116 ns respectively. As the longest-operating satellite clock, the overall fitting residuals for C01 are greater than the other two satellites, suggesting a higher noise level for C01 due to the long operating time and ageing components. In addition, the fitted residuals of the GEO and IGSO satellites are characterized by some cyclic variation with a period of about 51,840 s (180 days), while the MEO satellites do not have a significant long-term cyclic effect. This will be discussed in detail in Section 5.

There are obvious periodic terms in the low-frequency region of the spectrum, related to the satellite orbit position and diurnal changes. Meanwhile, some periodic terms with small amplitude in the high-frequency part belong to the noise caused by other factors, with the amplitude interrelated with the type of atomic clock. After being converted, the cycle terms of GEO and IGSO satellite clocks are mainly 24 h, 12 h, and 8 h, and the periodic terms of MEO are mainly 12.921 h and 6.458 h. The main period terms of clock noise are close to their earth orbit operation period or 1/2 times the period. That is, the satellite atomic clock period term is slightly larger than the period of satellite orbit: 23.935 h for GEO/IGSO and 12.887 h for MEO satellite orbit. The reason is that the solar perturbation change caused by the orbit operation has a periodic impact on the operation of the satellite clock. In addition, J2 relativity is also an important reason for the periodic term [29]. The

periodic terms of atomic clocks on different satellites in the same orbit are also different, which should be caused by other environmental noise.

4.2. Frequency Drift Rate

The frequency drift rate of the BDS satellite clock was calculated by Equation (6), and the average RMS value of the drift rate sequence was determined. Figure 7 shows the drift rate calculated by all satellite atomic clocks day by day; some detailed dynamic changes can also be observed.

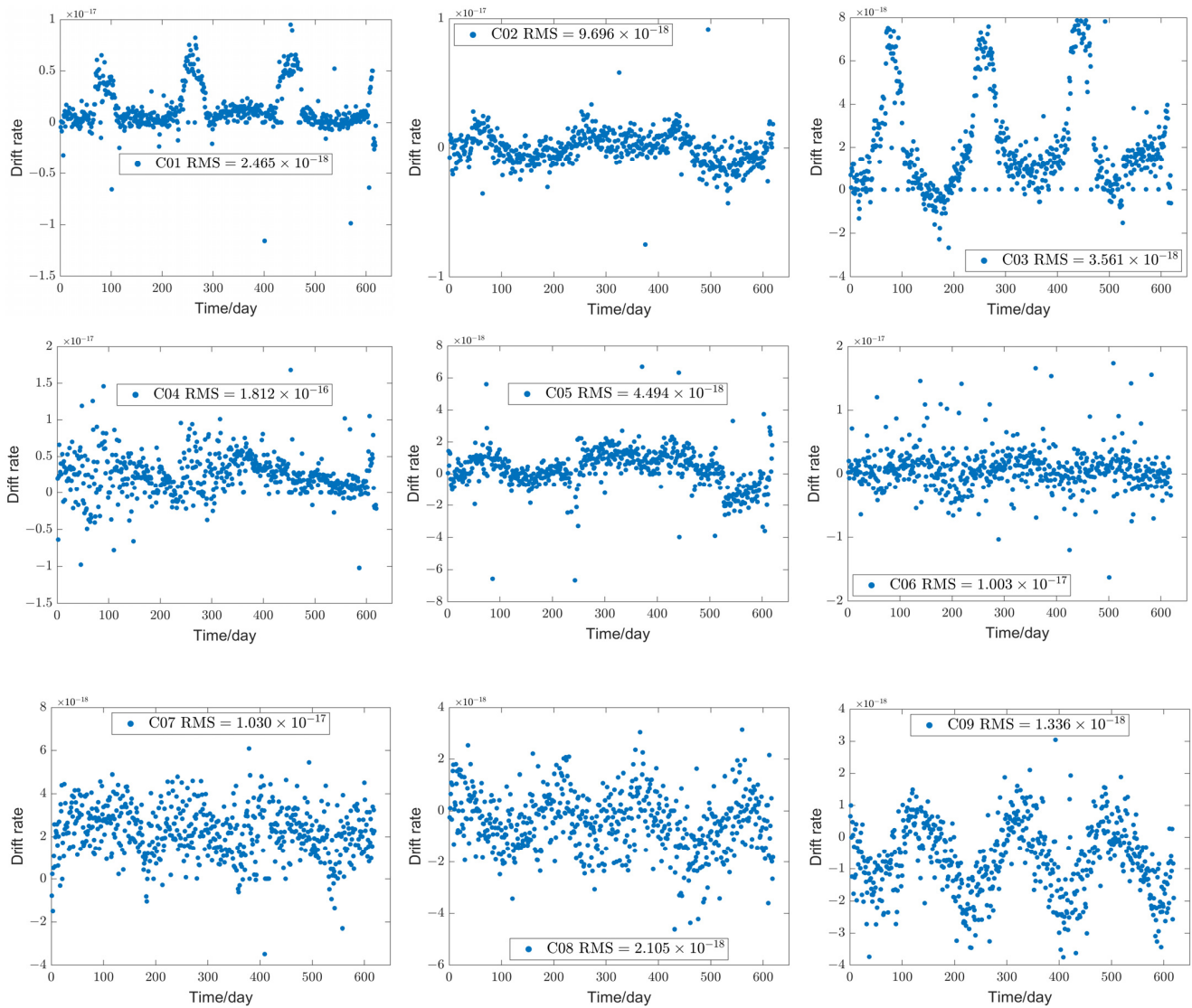


Figure 7. Cont.

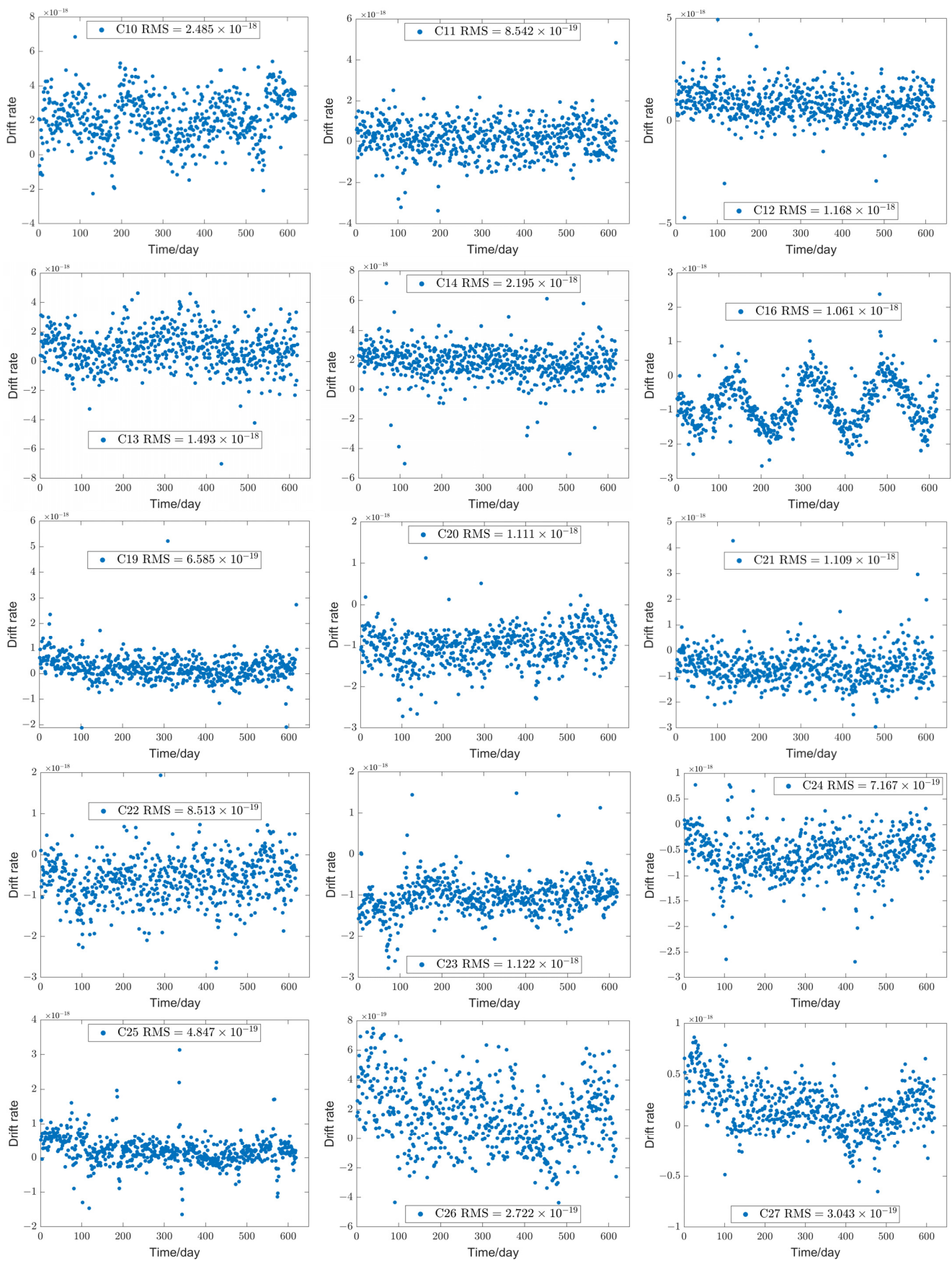


Figure 7. Cont.

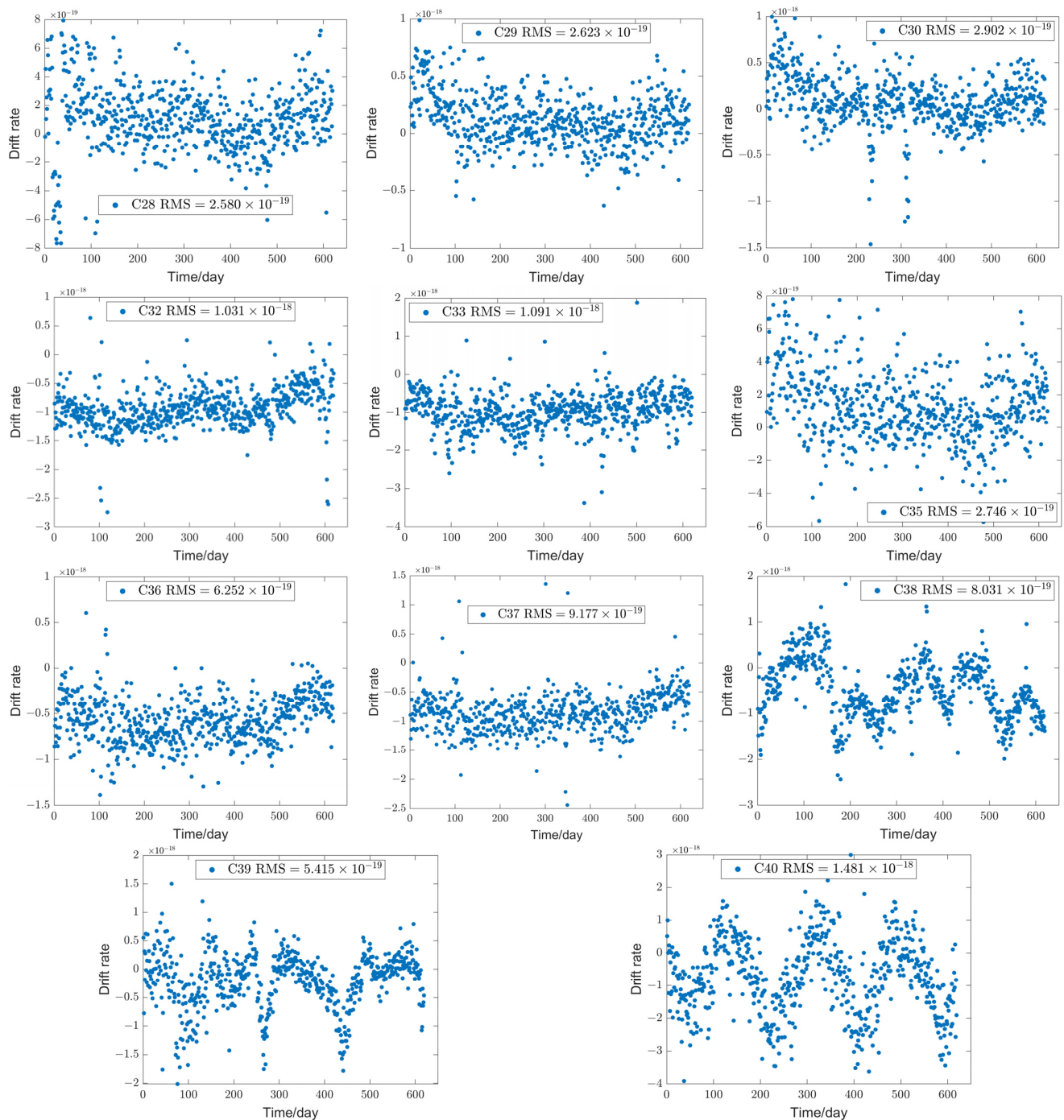


Figure 7. Drift rate of BDS satellite clocks.

Intuitively, the drift rate of a BDS-2 satellite atomic clock is generally in the order of 10^{-18} , while BDS-3 reaches the order of 10^{-19} . The C04 satellite with a long running time has the worst drift rate of 1.82×10^{-17} , which is due to the high drift rate caused by the ageing of the equipment of the satellite atomic clock after long-term operation. Comparison between different orbits shows that MEO satellite atomic clocks have the optimal drift rate; comparison between different clock types shows that PHM with the smooth trend has a better drift rate than RAFS. In addition, if there are some points with a relatively high drift rate (such as C30) in the overall drift change map curve, there will be fluctuation points at the corresponding position of the frequency map that protrude, which may be due to

the calculating error of the satellite clock offset or the switching between the primary and standby atomic clocks.

It is worth noting that the frequency drift of all GEO satellite clocks has the characteristics of oscillation and fluctuation; in addition, the frequency drift change of all IGSO satellite clocks is similar to the triangular wave law, with the cycle of half a year, which may be due to the slow change of frequency drift caused by the earth's movement. The daily frequency drift rate of the BDS satellite clock was calculated by Equation (6), and the average RMS value of the daily drift rate sequence was determined. Figure 8 shows the daily drift rate calculated by all satellite atomic clocks; some detailed dynamic changes could also be observed intuitively.

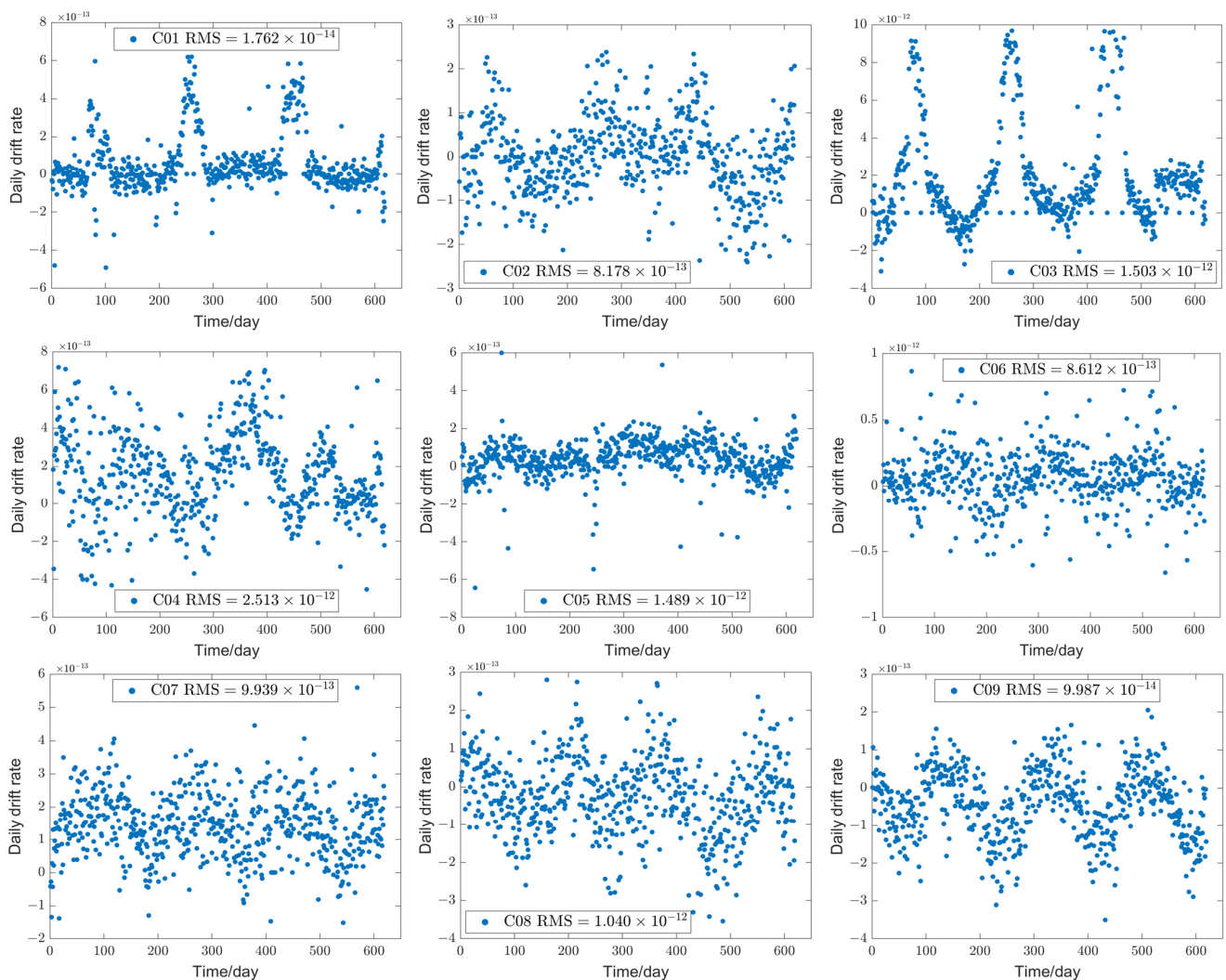


Figure 8. Cont.

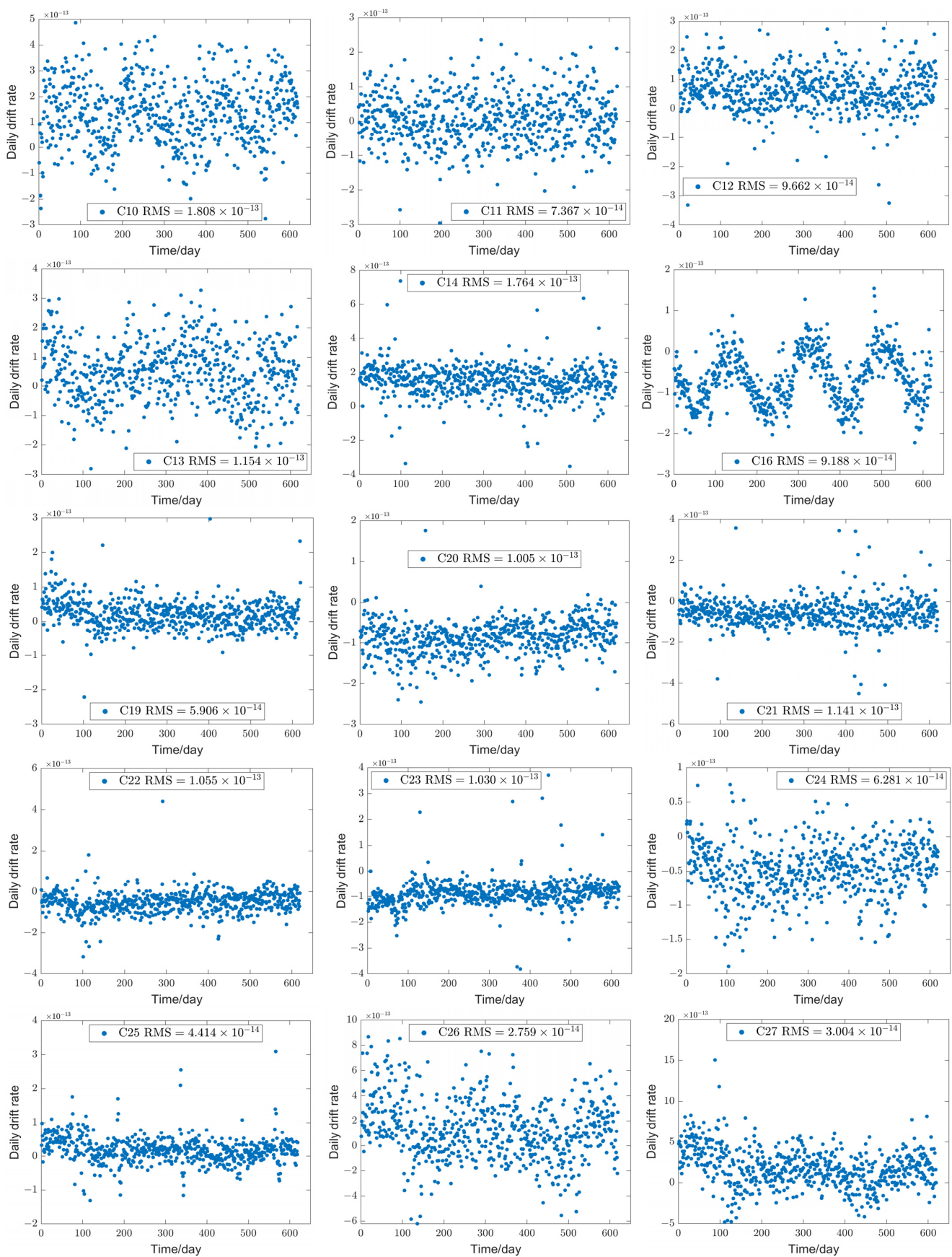


Figure 8. Cont.

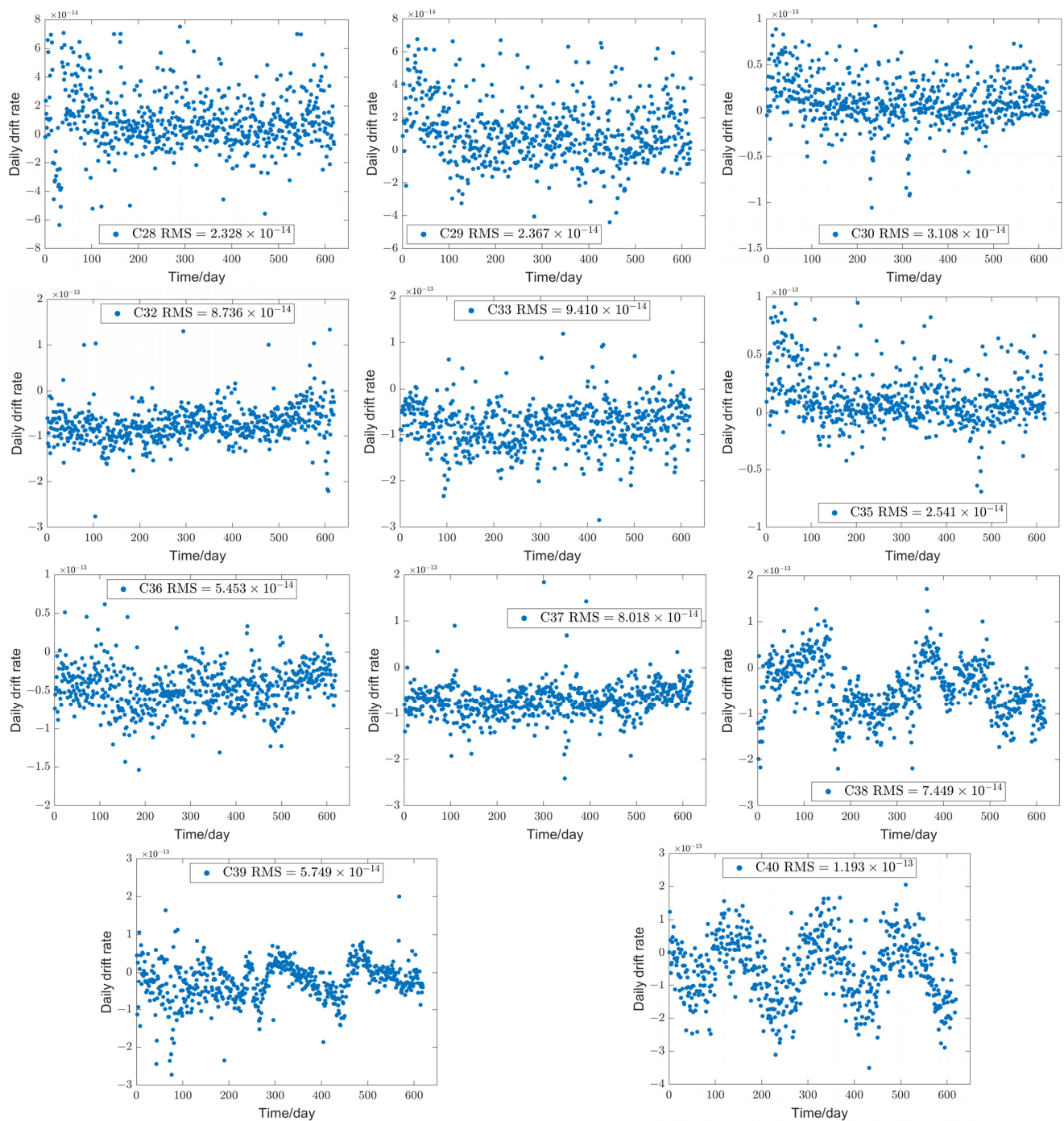


Figure 8. Daily drift rate of BDS satellite clocks.

Figure 8 shows that the daily drift rate shows similar characteristics to the drift rate in the same sampling period, and the relatively large fluctuation points in the drift rate graph are also reflected in the statistical graph of the daily drift rate. It is easy to find that the magnitude of PHM is better than the RAFS in terms of the performance of the daily drift rate, which also confirms that the PHM has superior long-term function. According to all the satellite data, the drift rate of each satellite clock does not show an obvious divergence trend after the long-term operation of the satellite, which proves that the phase and frequency adjustment and calibration operations after comparison with the time reference of the ground station are effective in restraining the drift speed of the satellite clock, especially for

the RAFS with a large long-term drift index. At present, although the drift rate index of BDS-2 satellite clocks is relatively inferior to BDS-3, its operation state is stable.

4.3. Frequency Accuracy

The frequency accuracy sequence was calculated by Equation (7), with days as the sampling time interval, and the average RMS value of the frequency accuracy was determined.

It can be seen from Figure 9 that the calculation result of frequency accuracy of atomic clock of each satellite is close to the output frequency value, but in fact, the influence of individual small fluctuations is excluded, which highlights the overall change trend. According to the calculation results, the frequency accuracy of the BDS-2 satellite clock is generally in the order of 10^{-11} , and the frequency accuracy of C04 is the worst, with an RMS of 1.66×10^{-10} . The frequency accuracy of the BDS-3 satellite atomic clock is mainly in the order of 10^{-12} , or even reaching the order of 10^{-13} . The PHM has better continuity and a smaller fluctuation range than the RAFS, and its change tends to be linear.

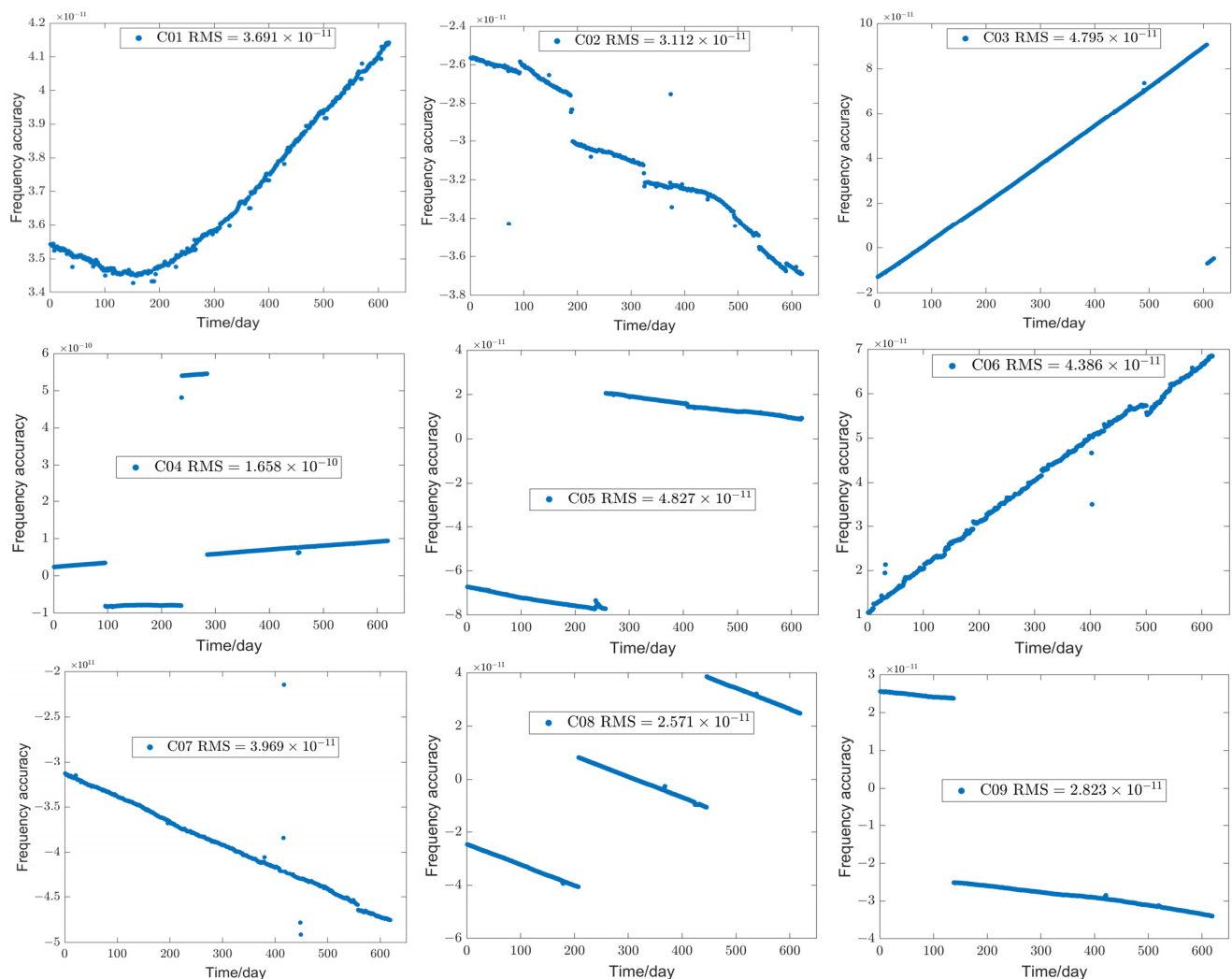


Figure 9. Cont.

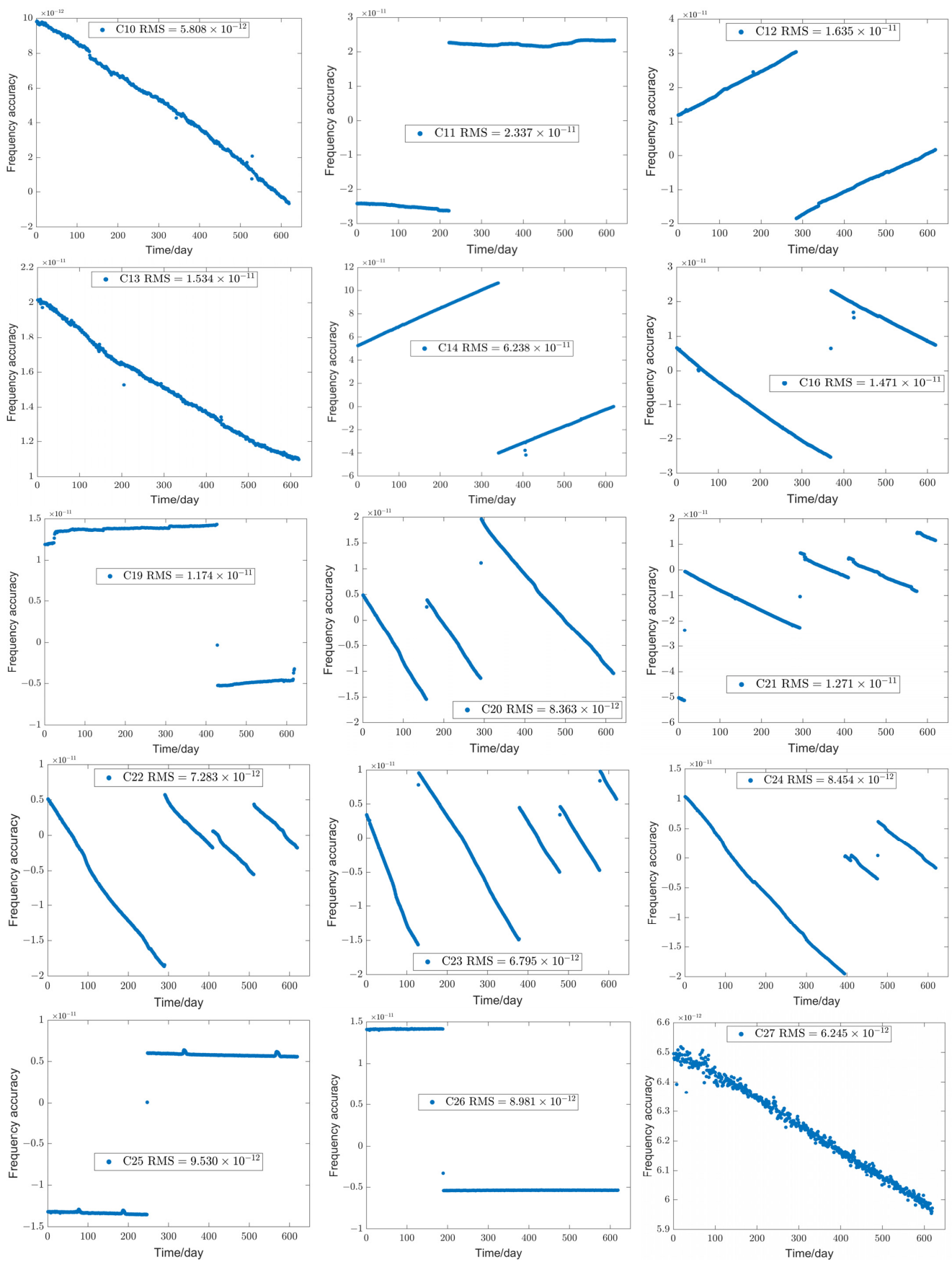


Figure 9. Cont.

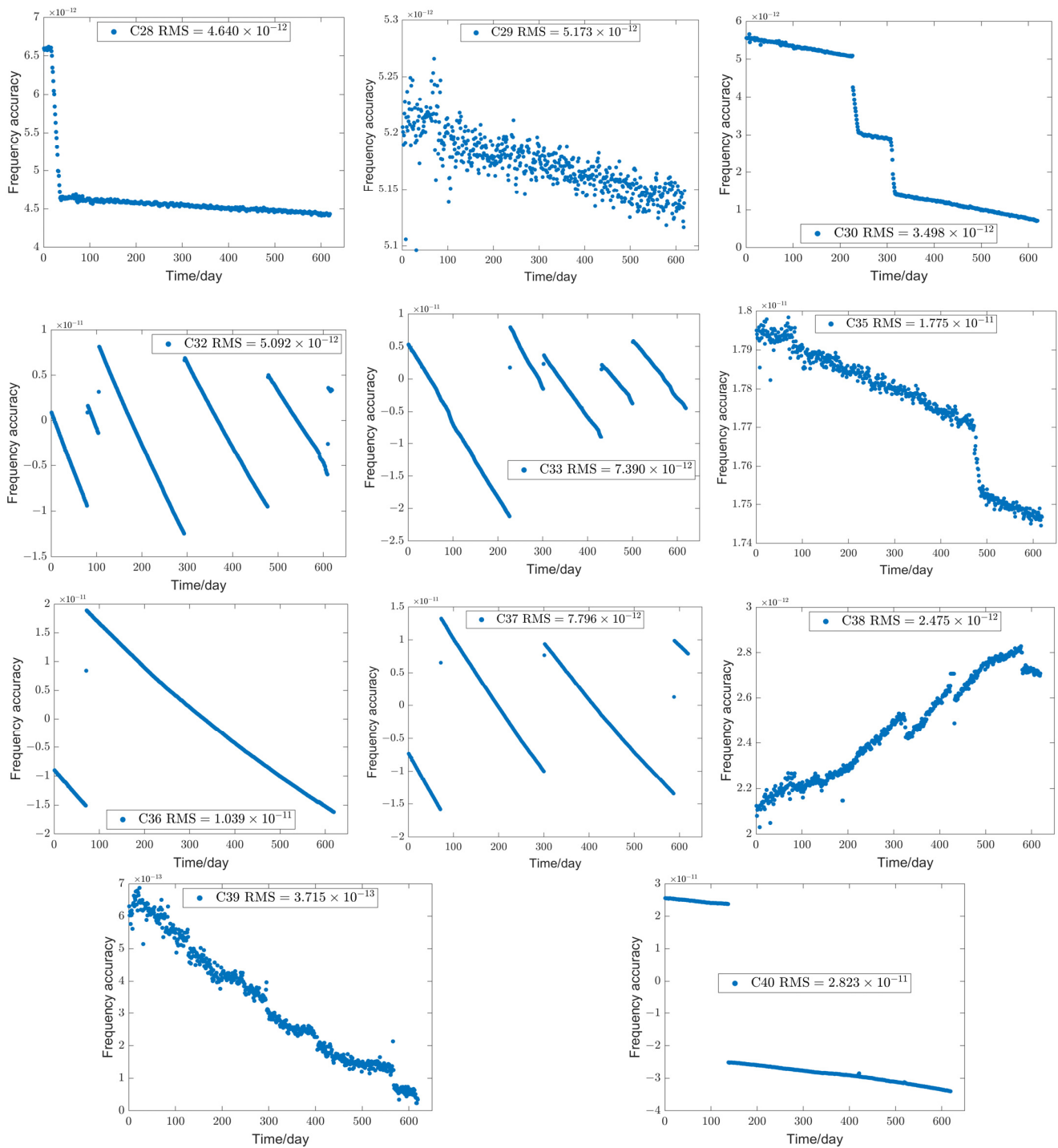


Figure 9. Frequency accuracy of BDS Satellites.

4.4. Frequency Stability

The overlapping Hadamard deviation was applied to the frequency stability calculation. The phase data of a single day were used to calculate the stability of 10,000 s, and the phase data of 15 consecutive days were used to calculate the stability of a day. The average indicators obtained for each month are shown in Figure 10.

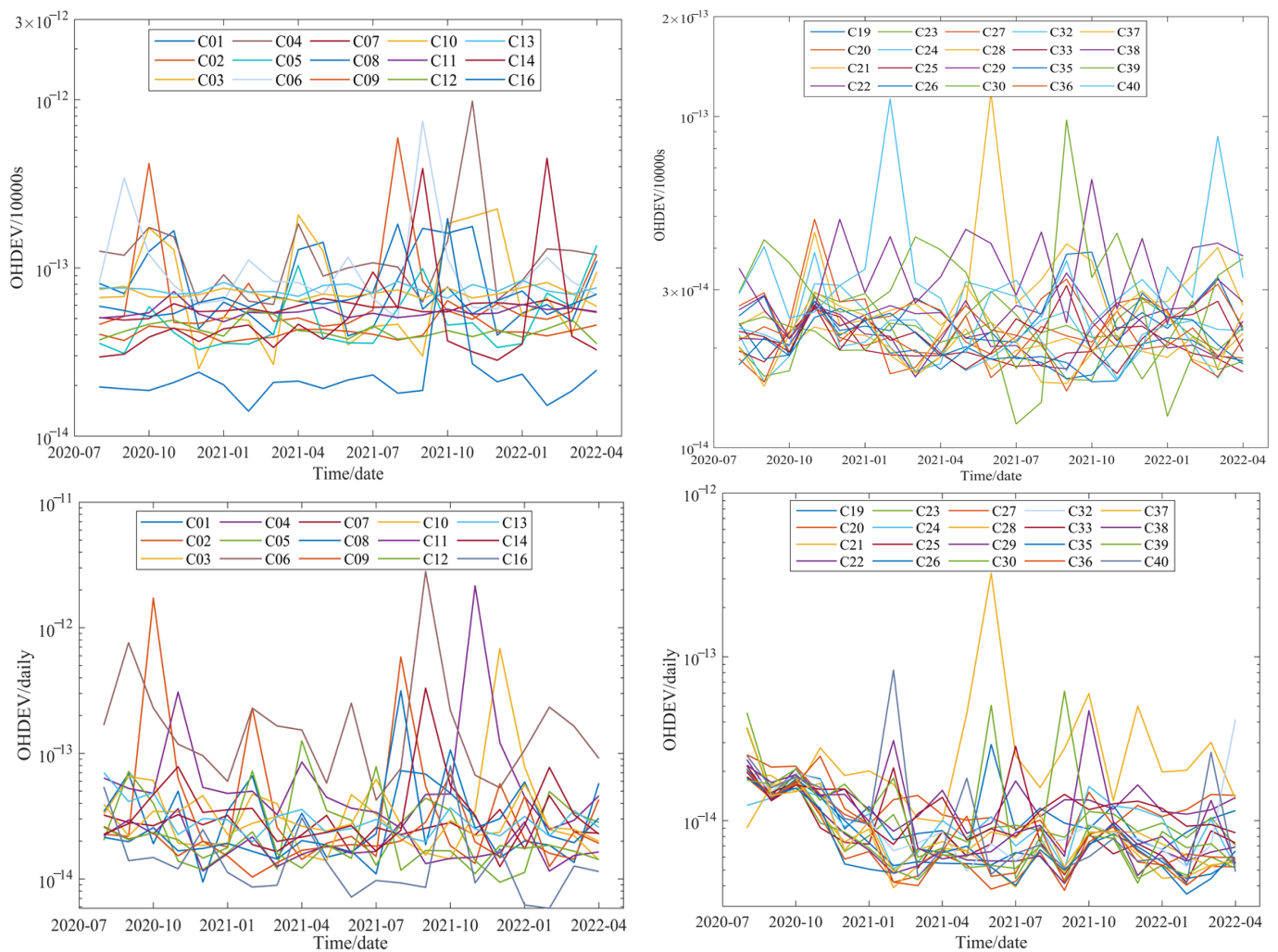


Figure 10. Sequence diagram of frequency daily stability.

The average frequency stability for 10,000 s of BDS-2 satellite atomic clocks is 7.53×10^{-14} , where C16 shows the best performance, reaching 2.88×10^{-14} , and satellite atomic clocks with a later launch time usually show performance superior to those with an earlier orbit. The average index of the BDS-3 satellite atomic clock is 2.48×10^{-14} , which is stable and maintained at a high level, and the performance has been significantly improved with time. In general, the frequency stability of BDS-2 satellite atomic clocks fluctuates significantly; a few satellite atomic clocks such as C02, C04, and C06 even have indicators inferior to 9.0×10^{-13} in some months. In contrast, the frequency stability of the BDS-3 satellite atomic clock fluctuates slightly, basically within the order of 10^{-14} .

The average frequency daily stability of BDS-2 satellite atomic clocks is 6.57×10^{-14} ; there are great distinctions between different clocks. A few satellite atomic clocks such as C09, C11, and C16 could reach the target superior to 2.0×10^{-14} , while the daily stability of C02, C04, and C06 is even inferior to their frequency stability for 10,000 s. This indicates that the long-term stability of satellite atomic clocks operating for more than 11 years will be significantly reduced, and the clock offset data solution strategy will also have an impact on the stability analysis. The daily frequency stability of BDS-3 satellite atomic clocks reached 1.19×10^{-14} on average; the stability of all clocks is reliable, with an index superior to 9.0×10^{-14} for every month. In terms of clock type, the daily stability of some BDS-3 RAFS has reached the level of 10^{-15} , and almost all PHMs have reached this accuracy.

In general, the frequency stability of BDS-3 satellite atomic clocks with a smaller fluctuation range is significantly superior to that of BDS-2, especially when the smoothing

time becomes longer. Dynamic changes indicate that the value of overlapping Hadamard variance shows a downward trend, especially for clocks launched at the later stage of BDS-3. In the first test month, the stability indicators of BDS-2 were mostly concentrated in the interval of $2\sim 7 \times 10^{-14}$, and then rose to $1\sim 4 \times 10^{-14}$ after 6 months; the corresponding indicators of BDS-3 are 2×10^{-14} and $3\sim 8 \times 10^{-15}$, respectively. Obviously, after the BDS was officially commissioned, it went through a period of testing and performance improvement for about half a year, so that the stability of the satellite atomic clock became better over time. As of 2021, the performance of BDS satellite atomic clocks has begun to be at a stable high level, mainly benefitting from the contributions of inter-satellite link measurements for the precise orbits and clock determinations of BDS-3 satellites [30,31].

5. Summary Analysis

For further comparative analysis and detailed discussion, the main indicators of each satellite atomic clock are listed in Table 2, and the corresponding main features of each stage are analyzed as follows:

- (1) Data quality. The MAD-based method is effective in processing a large number of satellite atomic clock offset data. The error rate of the original data of satellites launched by BDS-2 in the early stage was unacceptable, which reflects that the operating life would be exhausted. Similarly, the data efficiency of satellite clocks launched in the later stage was low, which was caused by the commissioning phase and would be improved when entering the stable operation stage.
- (2) Fitting residuals and periodic characteristics. The daily fitting residual of the BDS-2 satellite clock is within the range of 0.25–0.6 ns, while that of BDS-3 is in the range of 0.1–0.2 ns. The daily fitting residual is processed by FFT, and the main period terms of the satellite atomic clock obtained are close to 1 time or 1/2 of its orbital period. Specifically, 24 h and 12 h for Geo and IGSO and 12.92 h and 6.46 h for MEO, where the main period term of the orbital period is related to the influence of diurnal variation and solar light pressure, or it is related to the periodic change of the distance between the satellite and the earth during the elliptical orbit of the satellite (one circle around the earth must undergo two semi major axis and semi minor axis changes). In addition, the fitting residuals of the atomic clocks of GEO and IGSO satellites show a periodic variation law of about half a year, which may be related to the earth's revolution.
- (3) Frequency drift rate. The early BDS-2 satellite atomic clock has a large drift rate due to long service life, with more frequency modulation points and phase modulation points. The drift rate of RAFS launched at the later stage is at the same level as that of BDS-3, and the drift rate of PHM is optimal, whose phase change tends to be linear over the whole sampling period. In addition, the drift rates of GEO and IGSO showed a significant periodic term variation trend of about half a year, which was similar to the variation characteristics of the fitting residuals.
- (4) Frequency accuracy. The frequency accuracy of the BDS-2 atomic clock is at the 10^{-11} level, while that of BDS-3 is at the 10^{-12} level. The PHM has better continuity and a smaller fluctuation range. The change of frequency accuracy within the sampling time tends to be linear, and is superior to that of RAFS.
- (5) Frequency stability. The stability of the BDS-2 satellite clock is half an order of magnitude inferior to that of BDS-3. In particular, the five satellites C01–C05, which have been in service for a long time, not only have a low overall frequency stability, but also have greater fluctuations than other satellite clocks. Among the three satellites with different orbits, MEO has the optimal frequency stability, followed by IGSO, whilst GEO has the worst performance. The average daily frequency stability of BDS-3 satellite atomic clocks was 1.19×10^{-14} over the whole test period, and increasing to $3\sim 8 \times 10^{-15}$ with the stable operation of the system.

Table 2. Summary of performance indexes of BDS satellite atomic clocks.

System	PRN	Drift Rate (10^{-18})	Daily Drift (10^{-14})	Accuracy (10^{-11})	Stability (10^{-14})	Daily Stability (10^{-14})	Residuals (ns)	Cycle 1 (h)	Cycle 2 (h)	Cycle 3 (h)
BDS-2	C01	2.46	17.62	3.69	9.07	3.42	0.47	12.08	24.00	8.02
	C02	9.70	81.78	3.11	10.03	14.40	0.37	24.07	12.02	8.01
	C03	3.56	150.29	4.79	9.22	6.29	0.45	24.02	12.07	8.03
	C04	18.12	251.26	16.58	14.96	16.20	0.59	24.00	12.00	8.00
	C05	4.49	148.90	4.83	5.28	3.17	0.33	24.00	12.00	6.00
	C06	10.03	86.12	4.39	12.61	29.30	0.47	24.00	12.00	8.00
	C07	10.30	99.39	3.97	5.75	2.64	0.56	24.00	12.00	8.00
	C08	2.11	103.99	2.57	6.79	4.07	0.41	24.00	12.00	6.00
	C09	1.34	9.99	2.82	4.25	2.23	0.34	24.00	12.00	8.00
	C10	2.48	18.08	0.58	7.05	3.06	0.53	24.00	12.00	6.00
	C11	0.85	7.37	2.34	5.49	1.89	0.35	27.94	12.92	6.46
	C12	1.17	9.66	1.64	4.29	2.27	0.27	12.92	28.34	6.46
	C13	1.49	11.54	1.53	7.47	3.09	0.54	24.00	12.00	6.00
	C14	2.19	17.64	6.24	7.77	4.78	0.25	12.92	6.46	28.34
	C16	1.06	9.19	1.47	2.88	1.76	0.26	24.00	12.00	8.00
	Mean		4.76	68.19	4.04	7.53	6.57	0.41	-	-
BDS-3	C19	0.66	5.91	1.17	2.59	1.18	0.16	12.92	6.46	4.27
	C20	1.11	10.05	0.84	2.48	1.31	0.17	12.92	6.46	4.29
	C21	1.11	11.41	1.27	3.33	3.82	0.21	12.92	6.46	4.29
	C22	0.85	10.55	0.73	2.59	1.35	0.19	12.92	6.46	4.29
	C23	1.12	10.30	0.68	2.25	1.14	0.13	6.46	12.92	4.30
	C24	0.72	6.28	0.85	2.37	0.99	0.14	12.92	6.46	4.30
	C25	0.48	4.41	0.95	2.01	1.00	0.12	6.46	12.92	12.02
	C26	0.27	2.76	0.90	2.01	0.81	0.11	12.92	6.46	12.02
	C27	0.30	3.00	0.62	2.13	0.73	0.12	6.46	12.92	4.30
	C28	0.26	2.33	0.46	2.04	0.75	0.13	6.46	12.92	4.30
	C29	0.26	2.37	0.52	2.18	0.80	0.13	6.46	12.92	4.30
	C30	0.29	3.11	0.35	2.16	1.07	0.13	6.46	12.92	4.30
	C32	1.03	8.74	0.51	2.24	1.10	0.14	6.46	12.92	4.30
	C33	1.09	9.41	0.74	2.22	1.20	0.15	12.92	6.46	28.34
	C35	0.27	2.54	1.78	2.12	0.76	0.14	12.92	6.46	28.34
	C36	0.63	5.45	1.04	2.30	0.91	0.12	6.46	12.92	4.30
	C37	0.92	8.02	0.78	2.22	0.99	0.12	6.46	4.30	12.92
	C38	0.80	7.45	0.25	3.58	1.30	0.26	8.00	24.00	12.00
	C39	0.54	5.75	0.04	3.27	1.24	0.25	24.00	12.00	8.00
	C40	1.48	11.93	2.82	3.53	1.39	0.30	24.00	8.00	12.00
Mean		0.71	6.59	0.86	2.48	1.19	0.16	-	-	-
All	Mean	2.73	37.39	2.22	4.64	3.50	0.27	-	-	-

The analysis in this paper, combined with existing research results, shows the PHMs of Galileo at the present stage have the best performance, and the performance of BDS-3 is also at the first-class level, close to GPS. Meanwhile, there is still room for further improvement [14].

6. Conclusions

In this study, the necessary for long-term characterization of the BDS-3 satellite clock was described, the clock offset model and the calculation of the main indicators were introduced, and a systematic long-term characterization scheme for the satellite clock was designed. The characteristics of 35 BDS satellites atomic clocks were analyzed based on 620 days of precision clock aberration data provided by GFZ since July 2020. The MAD-based outlier detection method was applied to ensure the quality of the clock aberration data, and then the fitting residuals of the clock aberration model and the corresponding

spectral characteristics were calculated. Long-term dynamic indices such as frequency drift rate, frequency accuracy, and frequency stability were derived, respectively.

The analysis shows that the BDS-3 satellite atomic clock offset contains cyclic terms that are closely related to orbital operations, with the main cyclic term typically approaching the orbital operation duration or 1/2. The frequency drift rate and frequency accuracy of the BDS-3 satellite atomic clocks are generally an order of magnitude superior to those of BDS-2, and the frequency stability is about half an order of magnitude higher. Detailed changes in a number of long-term metrics have been discussed, notably the fitting residuals and the cyclic characteristics in the frequency drift rate of about half a year, and the significant improvement in frequency stability since BDS-3 was officially commissioned. The main findings can provide a reference for technical research on GNSS system operation monitoring, satellite atomic clock offset forecasting, and GNSS time scale algorithms.

Author Contributions: Y.L. and F.L. conceived and designed the experiments; Y.L. performed the experiments, analyzed the data, and wrote the paper; J.X. and M.W. helped in the discussion and revision; Y.L. completed the software code part to analyze the data. All authors have read and agreed to the published version of the manuscript.

Funding: This work was supported by the National Natural Science Foundation of China (No. 41804076 and 61503404).

Data Availability Statement: The datasets analyzed in this study are managed by IGS.

Acknowledgments: All authors gratefully acknowledge Deutsches geoforschungs zentrum and IGS for providing the data, mainly including clock and precise orbit determination data.

Conflicts of Interest: The authors declare no conflict of interest.

References

- Xu, X.; Li, M.; Li, W.; Liu, J. Performance Analysis of Beidou-2/Beidou-3e Combined Solution with Emphasis on Precise Orbit Determination and Precise Point Positioning. *Sensors* **2018**, *18*, 135. [CrossRef] [PubMed]
- Wang, M.; Wang, J.; Dong, D.; Meng, L.; Chen, J.; Wang, A.; Cui, H. Performance of BDS-3: Satellite visibility and dilution of precision. *GPS Solut.* **2019**, *23*, 2. [CrossRef]
- Ly, Y.; Geng, T.; Zhao, Q.; Liu, J. Characteristics of BeiDou experimental satellite clocks. *Remote Sens.* **2018**, *10*, 1847. [CrossRef]
- Jaduszliwer, B.; Camparo, J. Past, present and future of atomic clocks for GNSS. *GPS Solut.* **2021**, *25*, 27. [CrossRef]
- Huang, G.; Yu, H.; Guo, H.; Zhang, J.; Fu, W.; Tian, J. Analysis of the Mid-long Term Characterization for BDS On-orbit Satellite Clocks (in Chinese). *Geomat. Inf. Sci. Wuhan Univ.* **2017**, *42*, 982–988.
- China's BeiDou Navigation Satellite System. (GEO/IGSO/MEO). Available online: <http://www.BeiDou.gov.cn/xt/gfxz/201712/P020171221333863515306.pdf> (accessed on 2 August 2022).
- Zha, J.; Zhang, B.; Liu, T.; Hou, P. Ionosphere-weighted undifferenced and uncombined PPP-RTK: Theoretical models and experimental results. *GPS Solut.* **2021**, *25*, 135. [CrossRef]
- Zhang, B.; Chen, Y.; Yuan, Y. PPP-RTK based on undifferenced and uncombined observations: Theoretical and practical aspects. *J. Geod.* **2019**, *93*, 1011–1024. [CrossRef]
- Zhang, B.; Teunissen, P.J.G. Characterization of multi-GNSS between-receiver differential code biases using zero and short baselines. *Sci. Bull.* **2015**, *60*, 1840–1849. [CrossRef]
- Steigenberger, P.; Montenbruck, O. Galileo status: Orbits, clocks, and positioning. *GPS Solut.* **2017**, *21*, 319–331. [CrossRef]
- Xie, W.; Huang, G.; Wang, L.; Li, P.; Cui, B.; Wang, H.; Cao, Y. Long-term performance detection and evaluation of GLONASS onboard satellite clocks. *Measurement* **2021**, *175*, 109091. [CrossRef]
- Zaminpardaz, S.; Teunissen, P. Analysis of Galileo IOV + FOC signals and E5 RTK performance. *GPS Solut.* **2017**, *21*, 1855–1870. [CrossRef]
- Waller, P.; Gonzalez, F.; Binda, S.; Sesia, I.; Hidalgo, I.; Tobias, G.; Tavella, P. The In-Orbit performances of GIOVE clocks. *IEEE Trans. Ultras. Ferro. Freq. Cont.* **2010**, *57*, 738–745. [CrossRef] [PubMed]
- Wang, W.; Wang, Y.; Yu, C.; Xu, F.; Dou, X. Spaceborne atomic clock performance review of BDS-3 MEO satellites. *Measurement* **2021**, *175*, 109075. [CrossRef]
- Hauschild, A.; Montenbruck, O.; Sleewaegen, J.; Huisman, L.; Teunissen, P. Characterization of Compass M-1 signals. *GPS Solut.* **2011**, *16*, 117–126. [CrossRef]
- Wang, B.; Lou, Y.; Liu, J.; Zhao, Q.; Su, X. Analysis of BDS satellite clocks in orbit. *GPS Solut.* **2016**, *20*, 783–794. [CrossRef]
- Xie, X.; Geng, T.; Zhao, Q.; Liu, J.; Wang, B. Performance of BDS-3: Measurement Quality Analysis, Precise Orbit and Clock Determination. *Sensors* **2017**, *17*, 1233. [CrossRef] [PubMed]

18. Zhao, Q.; Wang, C.; Guo, J.; Wang, B.; Liu, J. Precise orbit and clock determination for BeiDou-3 experimental satellites with yaw attitude analysis. *GPS Solut.* **2017**, *22*, 367. [[CrossRef](#)]
19. Wu, Z.; Zhou, S.; Hu, X.; Liu, L.; Shuai, T. Performance of the BDS3 experimental satellite passive hydrogen maser. *GPS Solut.* **2018**, *22*, 647. [[CrossRef](#)]
20. Yan, X.; Huang, G.; Zhang, Q.; Liu, C.; Wang, L.; Qin, Z. Early analysis of precise orbit and clock offset determination for the satellites of the global BeiDou-3 system. *Adv. Space Res.* **2019**, *63*, 1270–1279. [[CrossRef](#)]
21. Xu, X.; Wang, X.; Liu, J.; Zhao, Q. Characteristics of BD3 Global Service Satellites: POD, Open Service Signal and Atomic Clock Performance. *Remote Sens.* **2019**, *11*, 1559. [[CrossRef](#)]
22. Montenbruck, O.; Steigenberger, P.; Prange, L.; Deng, Z.; Zhao, Q.; Perosanz, F.; Romero, I.; Noll, C.; Stuerze, A.; Weber, G. The Multi-GNSS Experiment (MGEX) of the International GNSS Service (IGS)- Achievements, prospects and challenges. *Adv. Space Res.* **2017**, *59*, 1671–1697. [[CrossRef](#)]
23. Gu, S.; Mao, F.; Gong, X.; Lou, L.; Xu, X.; Zhou, Y. Evaluation of BDS-2 and BDS-3 Satellite Atomic Clock Products and Their Effects on Positioning. *Remote Sens.* **2021**, *13*, 5041. [[CrossRef](#)]
24. Wu, Y.; Yang, B.; Xiao, S.; Wang, M. Atomic Clock Models and Frequency Stability Analyses. *Geomat. Inf. Sci. Wuhan Univ.* **2019**, *44*, 1226–1232.
25. Cao, X.; Kuang, K.; Ge, Y.; Shen, F.; Zhang, S.; Li, J. An efficient method for undifferenced BDS-2/BDS-3 high-rate clock estimation. *GPS Solut.* **2022**, *26*, 66. [[CrossRef](#)]
26. Huang, G.; Cui, B.; Xu, Y.; Zhang, Q. Characteristics and Performance Evaluation of Galileo On-orbit Satellites Atomic Clocks during 2014–2017. *Adv. Space Res.* **2018**, *63*, 2899–2911. [[CrossRef](#)]
27. Wu, W.; Guo, F.; Zheng, J. Analysis of Galileo signal-in-space range error and positioning performance during 2015–2018. *Satell. Navi.* **2020**, *1*, 6. [[CrossRef](#)]
28. Xie, W.; Huang, G.; Cui, B.; Li, P.; Cao, Y.; Wang, H.; Chen, Z.; Shao, B. Characteristics and performance evaluation of QZSS onboard satellite clocks. *Sensors* **2019**, *19*, 5147. [[CrossRef](#)]
29. Zhou, R.; Hu, Z.; Zhao, Q.; Li, P.; Wang, W.; He, C.; Cai, C.; Pan, Z. Elevation-dependent pseudorange variation characteristics analysis for the new-generation BeiDou satellite navigation system. *GPS Solut.* **2018**, *22*, 60. [[CrossRef](#)]
30. Qin, W.; Ge, Y.; Wei, P.; Dai, P.; Yang, X. Assessment of the BDS-3 on-board clocks and their impact on the PPP time transfer performance. *Measurement* **2020**, *153*, 107356. [[CrossRef](#)]
31. Huang, C.; Cui, B.; Zhang, Q.; Li, P. Switching and Performance Variations of On-Orbit BDS Satellite Clocks. *Adv. Space Res.* **2018**, *10*, 47. [[CrossRef](#)]